Available online at www.sciencedirect.com
SCIENCE DIRECT®
Earth and Planetary Science Letters 248 (2006) 495–507
EPSL
www.elsevier.com/locate/epsl

Reconstruction of regional atmospheric circulation features during the late Pleistocene in subtropical Brazil from oxygen isotope composition of speleothems

F.W. Cruz Jr. [a,b,*], S.J. Burns [a], I. Karmann [b], W.D. Sharp [c], M. Vuille [a]

[a] Department of Geosciences, Morrill Science Center, University of Massachusetts, Amherst, MA 01003, USA
[b] Instituto de Geociências, Universidade de São Paulo, Rua do Lago, 562, CEP 05508-080, São Paulo-SP, Brazil
[c] Berkeley Geochronology Center, 2455 Ridge Road, Berkeley, CA 94709, USA

Received 4 November 2005; received in revised form 9 June 2006; accepted 9 June 2006
Available online 14 July 2006
Editor: R.D. van der Hilst

Abstract

Two high-resolution oxygen isotope records of speleothems from caves located in subtropical Brazil provide a broad view of regional climate variations and related forcing during the late Pleistocene and Holocene. Here, we present a new record precisely dated by U-series extending back to 131 kyr BP from a speleothem collected in Santana Cave. Comparison with the 116 kyr BP record from Botuverá Cave confirms that the seasonal change in regional rainfall distribution is primarily controlled by variations in summer insolation on Milankovitch timescales. However, significant negative anomalies of $\delta^{18}O$ from 60 kyr BP to 10 kyr BP in the records suggest that the Northern Hemisphere glacial boundary conditions, in particular Heinrich events, impacted the mean location and/or convective activity of the South American summer monsoon (SASM), resulting in enhanced transport of depleted moisture from the Amazon Basin into the region. In addition, comparison of the two records indicates a steep north–south gradient in $\delta^{18}O$ of rainfall throughout, which is interpreted as reflecting different relative contribution of extratropical and monsoonal precipitation to the two locations. For some time periods, more pronounced negative $\delta^{18}O$ anomalies occur in the northern part and more positive anomalies in the southern part of the region, which appear to be associated with more abundant monsoonal and extratropical rainfall, respectively. The last interglacial period is characterized by the highest $\delta^{18}O$ values in the entire St8 record, indicating a dominance of extratropical winter rainfall and thus, the most northward position of the summer SASM for the last 131 kyr BP.

Keywords: speleothems; paleoclimate; insolation; stable isotopes; Brazil; last interglacial

1. Introduction

The subtropical Atlantic coast in Brazil is an excellent location for investigating past changes in the atmospheric circulation because it is a region where tropical and extratropical air masses intensely interact. Such interactions

* Corresponding author. Department of Geosciences, Morrill Science Center, University of Massachusetts, Amherst, MA 01003, USA. Tel./fax: +1 413 545 0659.
E-mail address: fdacruz@geo.umass.edu (F.W. Cruz).

0012-821X/$ - see front matter © 2006 Elsevier B.V. All rights reserved.
doi:10.1016/j.epsl.2006.06.019

are faithfully recorded in speleothems [1]. Reconstructing atmospheric circulation is possible because the $\delta^{18}O$ of rainfall, cave drip waters and related speleothems reflect primarily regional changes in the relative contributions of two moisture sources, isotopically enriched winter versus isotopically depleted summer rainfall. On an annual basis, the change from summer to winter moisture sources is due to a seasonal shift from a more monsoonal regime in summer to a more extratropical regime in winter. On longer timescales, changes in speleothem $\delta^{18}O$ reflect changes in the mean location of and intensity of convection within the South American Summer Monsoon (SASM), which controls the amount of summer precipitation in the region [2].

The extratropical circulation regime is responsible for a significant fraction of the regional precipitation during the winter and early spring (May to September) as a result of migratory cyclones along the subtropical Atlantic coast [3,4]. These rainfall events show relatively high values of $\delta^{18}O$ because they incorporate a larger fraction of moisture derived from the neighboring Atlantic Ocean [2]. On the other hand, the warm-season precipitation from late September to April is associated with the activity of the South American Summer Monsoon (SASM; [5,6]). An important feature of the SASM is the South American Convergence Zone (SACZ), a NW–SE elongated band of enhanced convective activity emanating from the Amazon basin and extending into subtropical latitudes and over the Atlantic Coast (Fig. 1) during the peak of monsoon [7].

The SASM accounts for over 80% of the annual mean precipitation at the center of SACZ activity at about 23°S, over Rio de Janeiro city and for 50% of the total summertime precipitation south of 25°S along the coast [8]. The monsoonal rainfall exhibits relatively low values of $\delta^{18}O$ because it incorporates a higher fraction of depleted moisture that is transported from the distant Amazon Basin to the Brazilian subtropics [2] by the South American low-level jet [7]. In addition, the availability of depleted moisture from distal sources in this region tends to be proportional to the degree of rainout of ^{18}O over the Amazon Basin, which is enhanced during more intense phases of the SASM [9,10].

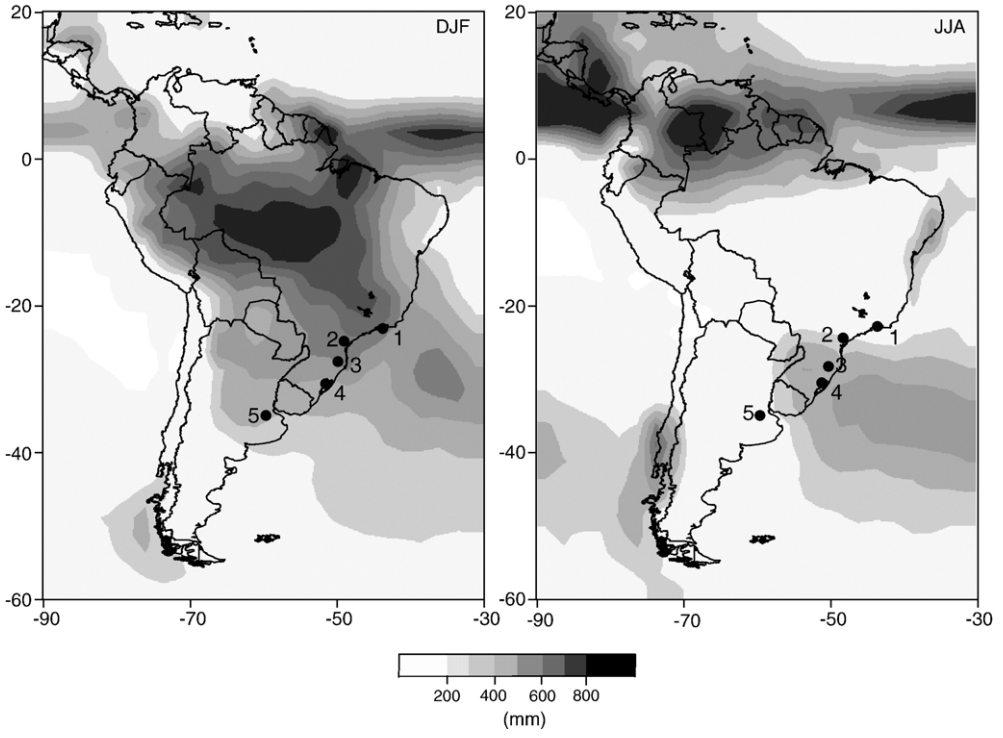

Fig. 1. Long-term mean (1979–2000) Climate Prediction Center Merged Analysis of Precipitation (CMAP, [28]) seasonal precipitation totals (in mm) for December–February (left) and June–August (right). Precipitation over SE Brazil in DJF is related to the southward expansion and intensification of the South American summer monsoon, while in JJA precipitation is of extratropical nature and associated with midlatitude cyclonic activity over the South Atlantic. Numbers in the figure indicate locations mentioned in text: 1 – IAEA station in Rio de Janeiro, Brazil; 2 – Santana cave; 3 – Botuverá Cave; 4 – IAEA station in Porto Alegre, Brazil; 5 – IAEA station in Buenos Aires, Argentina.

Large-scale processes within tropical and subtropical Brazil can influence modern precipitation climatology on distinct timescales, due to factors such as atmosphere–ocean interactions [11,12] and the intensity of the extra-tropical cold air incursions into the tropics [4,8]. During the late Pleistocene the moisture flux convergence and precipitation development is dominantly controlled by the amount of incoming summer solar radiation and to a lesser degree by millennial scale variations in the Northern Hemisphere [1]. However, a broader reconstruction of the regional circulation features in the past depends on comparisons between well-dated high-resolution records of paleoprecipitation. Here, we describe similarities and differences in the seasonal precipitation distribution over the past 131 kyr BP based on stable oxygen isotope records of speleothems from caves situated at ~24°S and ~27°S in subtropical Brazil. Comparison of the two records allows us to assess differences in the response of regional atmospheric circulation patterns to variations of precession-driven insolation versus remote forcings.

2. Study site, sample description and methods

This study used two speleothems collected in the Santana cave (St8, 24°31′51″S; 48°43′36″W) and one in the Botuverá cave (Bt2, 27°13′24″S; 49°09′20″W), which are located 300 km apart in southeastern and southern Brazil, respectively (Fig. 2). These caves are 6300 m and 1200 m long and were developed in low metamorphic grade limestones of the Meso to Neoproterozoic Açungui and Brusque Groups, respectively [13]. The present-day climate in both cave sites is sub-tropical humid, with nearly saturated mean relative humidity and rainfall that is uniformly distributed throughout the year [14]. The mean annual precipitation (MAP) from 1972 to 2004 at a meteorological station located 7 km from the entrance of Santana cave was 1589 mm (source DAEE: www.daee.sp.gov.br). MAP from 1911 to 1966 at a meteorological station 40 km from Botuverá Cave and at similar altitude was 1752 mm (source Climerh-Epagri, 2004, personal communication). The external mean annual temperatures (MATs) at Santana and Botuverá cave sites during 2000 and 2002 were 18.6 °C and 18.9 °C, respectively, in close agreement with measured internal MATs of 18.6 °C and 19.0 °C. The caves are located at the transition between the Atlantic coastal plain and the Brazilian plateaus: Santana cave is at an elevation of 550 m adjacent to the Serra do Mar and Botuverá cave at 250 m adjacent to Serra Geral (Fig. 2). Dense, tropical Atlantic rainforest and mature, clay-rich soils a few meters thick cover both areas.

St8 and Bt2 stalagmites are candle-like calcite stalagmites 167 cm and 70 cm tall, which were still active at the time of sampling (Fig. 3). They were collected at the end of each cave's main gallery and approximately 1500 m and 300 m from their only respective entrances and 300 and 110 m below the surface, respectively. The St8 age model is constrained by 31 ages measured at the Berkeley Geochronology Center (USA), using

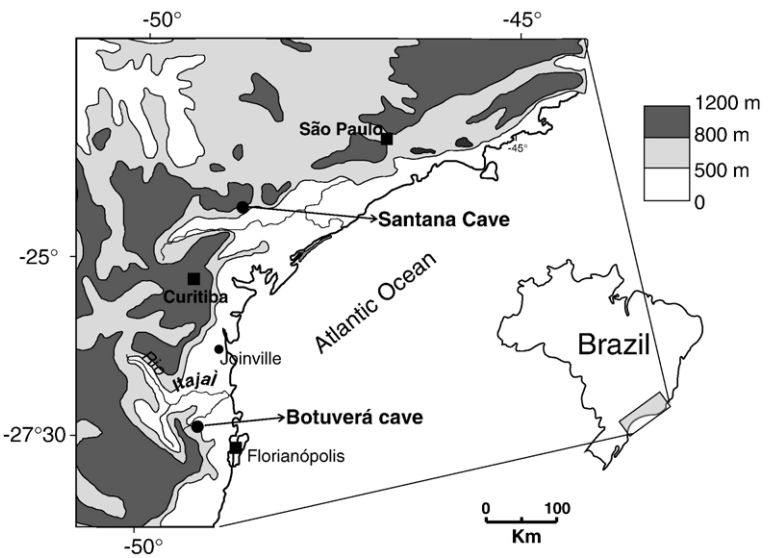

Fig. 2. Location map of the study sites in south and southeastern Brazil. Botuverá and Santana caves are located at the transition between Atlantic coastal plain and the Serra do Mar and/or Serra Geral plateaus. The altitude at the surface above the caves varies from 230 to 700 m a.s.l.

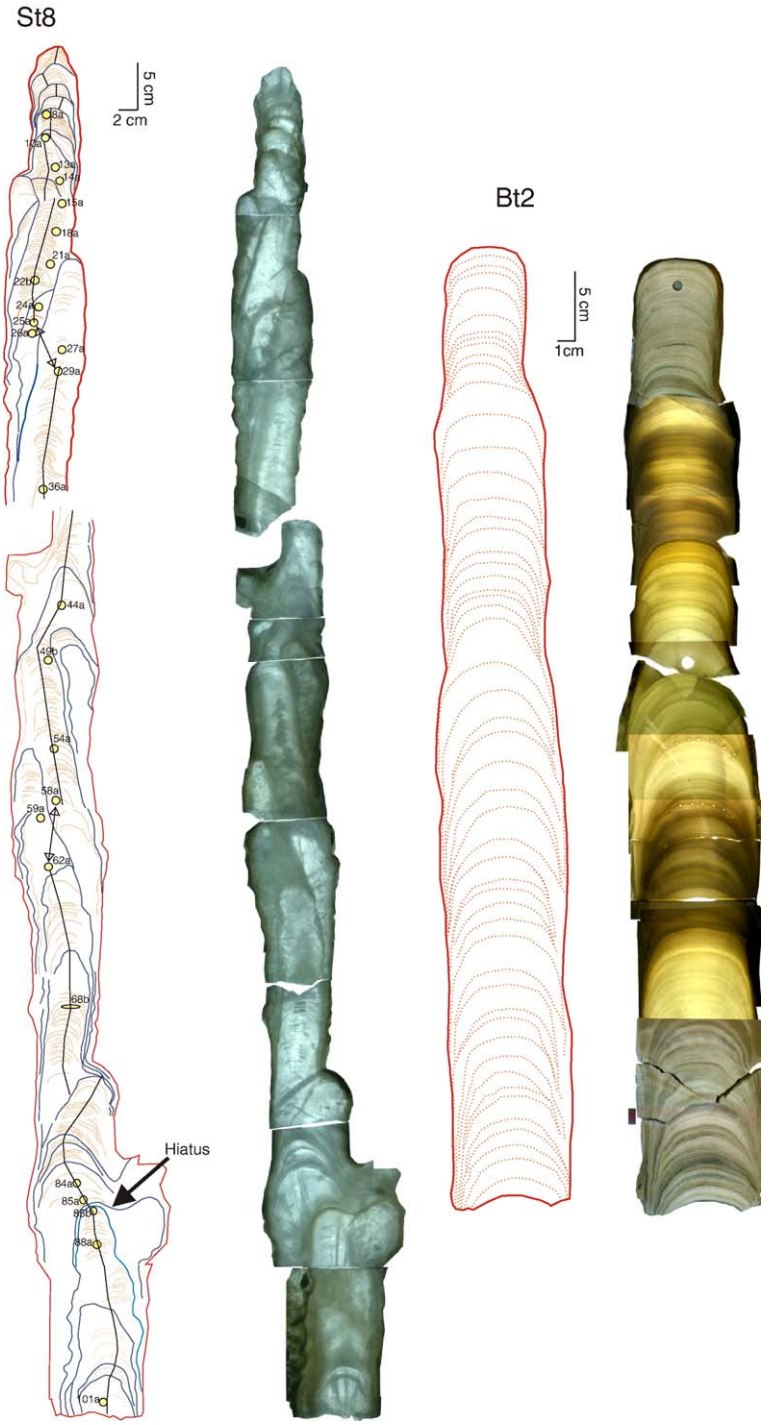

Fig. 3. Image and sketch of the St8 and Bt2 speleothems longitudinal slabs. The circles indicate the samples extracted for geochronology. St8 growth axis is indicated on the sketches with lines perpendicular to the speleothem laminations (subhorizontal concave lines).

conventional chemical and thermal ionization mass spectrometry (TIMS) techniques (Table 1; Fig. 4). Its stable oxygen isotope long-axis profile is based on 658 measurements performed at the University of Massachusetts. Samples preparation and experimental procedures used for both geochronology and stable oxygen and carbon isotopes analysis for St8 stalagmite was as described by Cruz et al. [1] for Bt2 sample. Both

Table 1
Dating results for speleothem St8

Sample	mm [a]	Wt. (mg)	U (ppm)	^{232}Th (ppb)	(^{230}Th/^{232}Th)	Measured		Detritus-corrected [b]		Age [c] (10^3 yr)	Initial [d] (^{234}U/^{238}U)
						(^{230}Th/^{238}U)	(^{234}U/^{238}U)	(^{230}Th/^{238}U)	(^{234}U/^{238}U)		
St8-8a	78	209.15	0.121	0.131	15.39	0.054±0.002	1.736±0.007	0.051±0.002	1.738±0.008	3.3±0.16	1.745±0.009
St8-10a	100.5	409.06	0.165	0.091	42.72	0.077±0.003	1.737±0.005	0.076±0.003	1.738±0.005	4.9±0.22	1.748±0.005
St8-13a	137.8	403.69	0.093	0.067	43.14	0.101±0.002	1.734±0.005	0.099±0.002	1.735±0.005	6.4±0.17	1.749±0.005
St8-14a	145.3	427.56	0.142	0.066	74.53	0.114±0.003	1.719±0.009	0.113±0.003	1.72±0.009	7.4±0.18	1.735±0.009
St8-15a	176.9	212.06	0.159	0.076	99.16	0.155±0.006	1.704±0.005	0.154±0.006	1.705±0.005	10.3±0.45	1.726±0.005
St8-18a	208.9	211.55	0.134	0.574	14.61	0.206±0.004	1.718±0.007	0.196±0.006	1.727±0.009	13.1±0.45	1.755±0.008
St8-21a	261	419.88	0.095	0.090	72.81	0.228±0.009	1.717±0.003	0.226±0.009	1.719±0.004	15.2±0.68	1.750±0.004
St8-22b	281	470.6	0.058	0.031	159.962	0.28±0.006	1.744±0.012	0.279±0.006	1.745±0.012	18.74±0.44	1.786±0.012
St8-24a	310.9	418.9	0.147	0.023	637.113	0.33±0.003	1.702±0.006	0.33±0.003	1.703±0.006	23.1±0.25	1.750±0.006
St8-25a	327	400	0.166	0.130	144.735	0.372±0.006	1.692±0.009	0.371±0.006	1.693±0.009	26.5±0.54	1.747±0.009
St8-26a	337.7	210.08	0.215	0.149	164.372	0.375±0.006	1.697±0.003	0.373±0.006	1.698±0.003	26.6±0.52	1.753±0.003
St8-27a	352	422.18	0.142	0.023	680.766	0.363±0.004	1.681±0.011	0.362±0.004	1.686±0.011	25.9±0.36	1.738±0.012
St8-29a	379.1	208.25	0.140	0.078	200.328	0.366±0.003	1.68±0.008	0.365±0.003	1.681±0.008	26.2±0.31	1.733±0.009
St8-36a	475.5	423.02	0.140	0.022	742.457	0.396±0.004	1.654±0.006	0.396±0.004	1.654±0.006	29.2±0.39	1.710±0.006
St8-40a	555.2	420.74	0.041	0.040	134.898	0.437±0.012	1.616±0.009	0.435±0.012	1.618±0.009	33.3±1.11	1.679±0.01
St8-44a	621	210.12	0.050	0.111	71.049	0.52±0.020	1.595±0.012	0.517±0.020	1.599±0.012	41.4±1.95	1.673±0.013
St8-49b	691	364.43	0.051	0.048	200.001	0.616±0.014	1.606±0.008	0.615±0.014	1.607±0.008	50.7±1.49	1.701±0.009
St8-54a	775	211.64	0.114	0.049	443.827	0.626±0.013	1.582±0.004	0.626±0.013	1.582±0.004	53.0±1.41	1.677±0.005
St8-58a	837	364.36	0.119	0.034	736.056	0.684±0.009	1.569±0.013	0.684±0.009	1.569±0.013	59.9±1.23	1.674±0.014
St8-59a	860	211.9	0.123	0.106	259.071	0.734±0.016	1.55±0.007	0.734±0.016	1.551±0.007	66.7±2.0	1.666±0.008
St8-62a	903	421.14	0.113	0.049	517.720	0.734±0.009	1.561±0.008	0.734±0.009	1.562±0.008	66.1±1.2	1.677±0.009
St8-68b	1053	421.03	0.14	0.037	896.2	0.804±0.007	1.548±0.006	0.804±0.007	1.549±0.006	75.6±0.9	1.680±0.006
St8-84a	1220	209.27	0.082	0.042	486.493	0.816±0.010	1.505±0.011	0.815±0.010	1.506±0.011	80.4±1.6	1.635±0.012
St8-85a	1240	415.26	0.12	0.031	982.7	0.861±0.011	1.513±0.014	0.86±0.010	1.513±0.014	86.2±2.0	1.655±0.016
St8-85b	1244	407.98	0.08	0.026	868.5	0.95±0.011	1.498±0.006	0.95±0.011	1.498±0.006	101.7±2.0	1.664±0.007
St8-88a	1274	419.97	0.096	0.038	742.045	0.968±0.014	1.482±0.005	0.968±0.014	1.482±0.005	106.6±2.5	1.653±0.007
St8-101a	1450	210.39	0.098	0.134	215.687	0.97±0.018	1.453±0.006	0.97±0.018	1.455±0.006	110.5±3.4	1.623±0.009
St8-102	1527.3	390.61	0.05	0.122	120.9	1.028±0.010	1.527±0.016	1.028±0.010	1.531±0.017	111.0±2.8	1.727±0.019
St8-103	1577	435.54	0.10	0.111	284.8	1.059±0.012	1.486±0.003	1.059±0.012	1.488±0.003	122.8±2.4	1.691±0.006
St8-104	1597.2	449.61	0.12	0.739	52.2	1.101±0.012	1.532±0.008	1.103±0.013	1.542±0.009	123.1±2.8	1.768±0.011
St8-105	1671	399.69	0.12	0.356	113.5	1.11±0.007	1.497±0.004	1.112±0.007	1.502±0.005	131.3±1.6	1.728±0.006

All ratios are activity ratios.
[a] Distance from the top of speleothem.
[b] Corrected for detrital U and Th with ^{232}Th/^{238}U=1.21±50%, ^{230}Th/^{238}U=1.0±10%, ^{234}U/^{238}U=1.0±10% (zero error correlations).
[c] The age uncertainties are at 95% confidence limits.
[d] Backcalculated from the present-day, detritus-corrected ^{234}U/^{238}U, and the ^{230}Th/U age.

stalagmites have an average resolution of ~150 yrs. Oxygen isotope ratios are expressed in δ notation, the per mil deviation from the VPDB standard.

The St8 stalagmite is entirely formed by transparent rombohedric calcite (confirmed by X-ray diffraction) with no clearly visible laminations and does not show evidence of secondary mineral alteration, such as corrosion features and recrystallization. Through transmitted light imaging of St8 it was possible to see a discrete banding, and pristine primary structures perpendicular to the growth axis (Fig. 3). St8 exhibits frequent shifts in growth axis direction caused by slight lateral dislocations of the drip point over the depositional surface. In addition, a complex pattern of parallel growth of two stalagmites was observed in some parts of the sample. The identification of these features was of great importance in delimiting the stable isotope profile and choosing representative samples for geochronology. For instance, areas showing contemporaneous parallel growth were identified in St8 between geochronology samples 25a to 29a and 58a to 62a and the continuity of the profile has been indicated by arrows in the stalagmite sketch (Fig. 3).

3. Results

3.1. Stable isotopic composition of precipitation; cave drip water and modern speleothems

Although stable oxygen isotope ratios in data from IAEA–GNIP stations along the Atlantic coast of South America between 23° and 34°S, in Rio de Janeiro, Porto

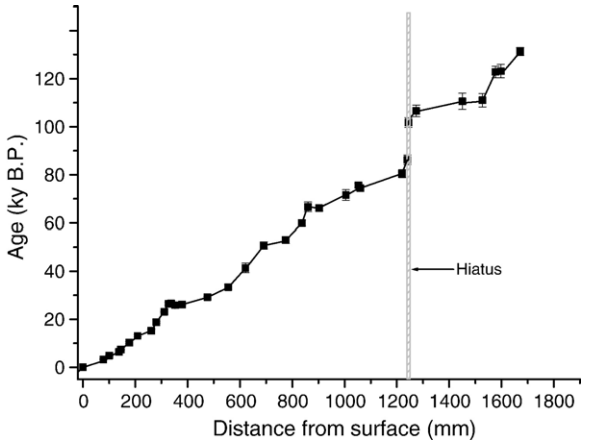

Fig. 4. Age versus depth model for stalagmite St8. Error bars are 95% confidence limits. The solid line connecting the data points is the linear interpolation used to calculate ages of individual oxygen isotope data points.

Alegre and Buenos Aires, reveal similarities among their isotopic variations, there are significant differences in the relative importance of factors controlling the regional rainfall isotopic composition (Figs. 1 and 5). The mean annual rainwater $\delta^{18}O$ value is −4.1‰ in Rio de Janeiro and −4.82‰ in both Porto Alegre and Buenos Aires Stations. The monthly variability is marked by more enriched values (between −4.5‰ to −2‰) from June to September and more depleted values (between −4.5‰ to −7.5‰) from December to May, respectively (Fig. 5; [15]). Nevertheless, the rainfall amount effect is only considered a dominant factor influencing the isotope signature of rainfall in Rio de Janeiro (23°S; [2]), where extratropical precipitation is almost negligible [4]. In contrast, the rainfall composition over the region farther to the south is mostly affected by the seasonal alternations in the relative contribution of local (more enriched) and distal (more depleted) moisture sources during the prevalence of extratropical and monsoonal rainfall regimes, respectively [2]. Furthermore, the influence of temperature variations on isotopic fractionation of rainfall is a minor factor, not just in the study region, but also over most of the continent [9].

Comparisons of cave waters and modern speleothems collected in Santana and Botuverá caves reveal a significant meridional gradient in the oxygen stable isotopic composition. The $\delta^{18}O$ of both water and speleothems from Botuverá are more enriched than those from Santana cave by approximately 1‰. The mean $\delta^{18}O$ values in the latter cave are −5.34±0.40‰ (SMOW, n=101) and −5.72±0.31‰ (PDB, n=19), while in the former cave they are −4.28±0.28‰ (SMOW, n=12) and −4.49±0.42‰ (PDB, n=12), for drip water and modern speleothems, respectively. These differences in $\delta^{18}O$ have been attributed to changes in the regional rainfall composition as evidenced by the monitoring program performed for soil and cave waters in Santana cave [2]. Results suggest that the more enriched values at Botuverá are due to a larger relative contribution of Atlantic moisture and less Amazonian moisture than at Santana. Botuverá has ~20% more precipitation during winter to early spring (July to September) and ~27% less during summer than Santana (December to February). Groundwater enrichment due to evaporation is unlikely to occur in soil surface or in galleries of Botuverá cave, because its geological/hydrological setting is similar to Santana and is situated in an even wetter area with no defined dry periods. Simultaneous and relatively rapid variations in $\delta^{18}O$ of water from soil and drip sites showing very contrasting mean discharges and located at depths from 100 m to 300 m in Santana Cave also revealed that

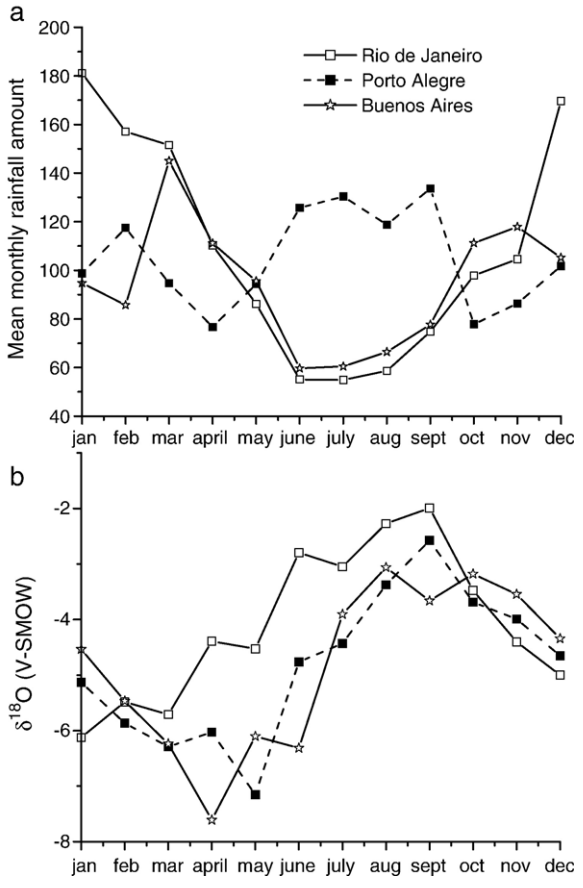

Fig. 5. Data from IAEA stations Rio de Janeiro, Porto Alegre and Buenos Aires [15], (a) monthly rainfall amount, (b) weight mean monthly $\delta^{18}O$.

processes like effective mixing between newly infiltrated and old waters stored in the aquifer above cave and CO_2 degassing are unlike to be a major factor affecting the isotopic composition of drip waters and consequently the calcite in stalagmites; otherwise different responses of infiltrated waters due to variations time of residence and rate of degassing should be expected between slow and fast dripping speleothems [2].

Contrary to expectations, the mean annual $\delta^{18}O$ at Rio de Janeiro station is slightly higher than at Porto Alegre, where extratropical precipitation dominates over monsoon-related precipitation [15]. This is likely because strong rainout over the Amazon basin will lead to residual water vapor which is more depleted in ^{18}O and hence the residual moisture could produce very depleted rains, even if the total precipitation is reduced [10]. Such a scenario could explain the depleted $\delta^{18}O$ values during the relatively dry months of March and April at Porto Alegre station (Fig. 5). According to Vuille and Werner [10], the degree of rainout during moisture transport is considered to be more important than the "rainfall amount effect" in this region so that very negative $\delta^{18}O$ values can result from an enhancement in the transport of distal moisture during a strong SASM. Therefore, we suggest that this mechanism produces the anomalously negative mean annual $\delta^{18}O$ values at Porto Alegre and the surrounding area. Hence the isotope ratios of cave drip waters capture the changes in the balance between the types of precipitation because they basically rely on the proportion of rainwater infiltrated from distinct seasons. Thus the apparent $\delta^{18}O$ gradient between Botuverá and Santana in both drip waters and modern speleothems is connected to the regional precipitation patterns and moisture sources.

3.2. Oxygen isotopic composition of fossil speleothems

The stable oxygen isotope profile of stalagmite St8 is presented in Fig. 6. The new $\delta^{18}O$ dataset of St8 stalagmite is detailed below and discussed later together with the previously published Bt2 stalagmite record [1]. St8 covers most of the last 131 kyr BP, except for the hiatus from 103 to 88 kyr BP, and includes much of the last interglacial phase, an interval that has not yet been documented in other paleoclimate studies of the region. The oxygen isotope ratios for stalagmite St8 range from −8.00‰ to −0.74‰ (mean value=−5.09‰) with an apparent cyclicity of ~20 kyr BP, which was also observed in the Bt2 record from Botuverá cave (Fig. 6). Despite the proximity of cave sites, there is a substantial difference in mean values between St8 records and Bt2 of about 2 ‰, with consistently higher $\delta^{18}O$ values in the latter.

Overall, the oxygen isotopic time series from stalagmites St8 and Bt2 are very similar (Fig. 6). In both records, a strong covariance with insolation can be observed, and much millennial-scale variability is also shared between the records. The good match between records indicates that the St8 age model is generally sound, despite the complex internal stratigraphy of this stalagmite. For one part of the St8 record, however, differences in the absolute age of the abrupt transition from more to less negative values at around 84 kyr BP, suggest that the St8 chronology may be affected by shifts in the growth axis position. We find it unlikely that a true age difference of several thousand years for this transition exists between the two records because they are only 300 km distant from one another. Other differences in the age models of the two records are within the errors of the measured age determinations.

The $\delta^{18}O$ values in St8 change in parallel with Southern Hemisphere summer insolation throughout the record. For the last 70 kyr BP, however, this cyclicity is not as well defined as in Bt2, especially during the positive phases of summer insolation. The highest $\delta^{18}O$ values occur at time intervals 131–113 kyr BP, 106–102 kyr BP, 81–77 kyr BP and during Holocene from 10 to 3 kyr BP, with the lowest $\delta^{18}O$ values occurring at present, 113–107 kyr BP, 67–60 kyr BP, 47–37 kyr BP and 20–15.5 kyr BP. Superimposed on the St8 20 kyr BP cycles are millennial to centennial $\delta^{18}O$ events, recognizable by fluctuations between 0.8‰ and 1.5‰ that are nearly coincident with variations seen in the Bt2 and also with Northern Hemisphere ice-core $\delta^{18}O$ records on the same timescale. However, some short-lived $\delta^{18}O$ peaks in Bt2 are not present in St8, such as those observed around 113 kyr BP, 65 kyr BP and less pronounced during the Bølling–Allerød (BA) event, at about 14 kyr BP (Fig. 6). On the other hand, the millennial scale lows in St8 are sometimes longer and more intense than in Bt2 as seen at around 56 kyr BP and during the equivalent of the Younger Dryas (YD) at about 12–11 kyr BP.

Fig. 7 shows the anomalies (record $\delta^{18}O$ mean-individual values) of the oxygen isotope ratios for both St8 and Bt2 compared with summer insolation at 30°S in order to provide a more realistic comparison of temporal variability between records. It is clear that both anomaly curves reproduce the overall pattern and amplitude of insolation but important differences remain. The anomalies in Bt2 match the amplitude of insolation remarkably well, with exception of rather negative anomalies at 47–40 kyr BP and 18–14 kyr BP and less positive anomalies at 34–27 kyr BP. Less agreement is observed from a similar comparison for St8, for example at 125–118 kyr BP and between 60 and 15 kyr BP. At the former

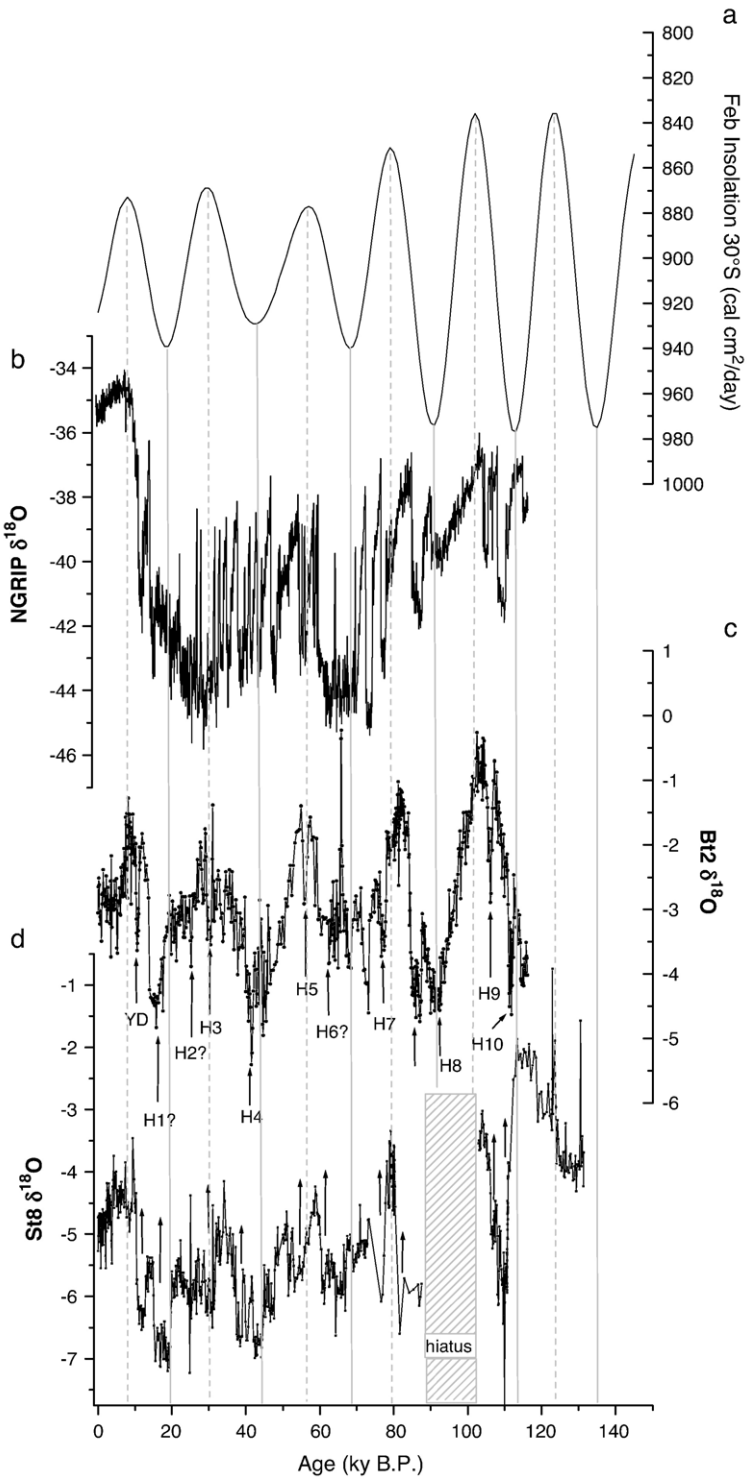

Fig. 6. Comparison between (a) February insolation at 30°S [29]; (b) oxygen isotopes of the NGRIP ice core from Greenland [30]; oxygen isotopes of Bt2 (c) and St8 (d).

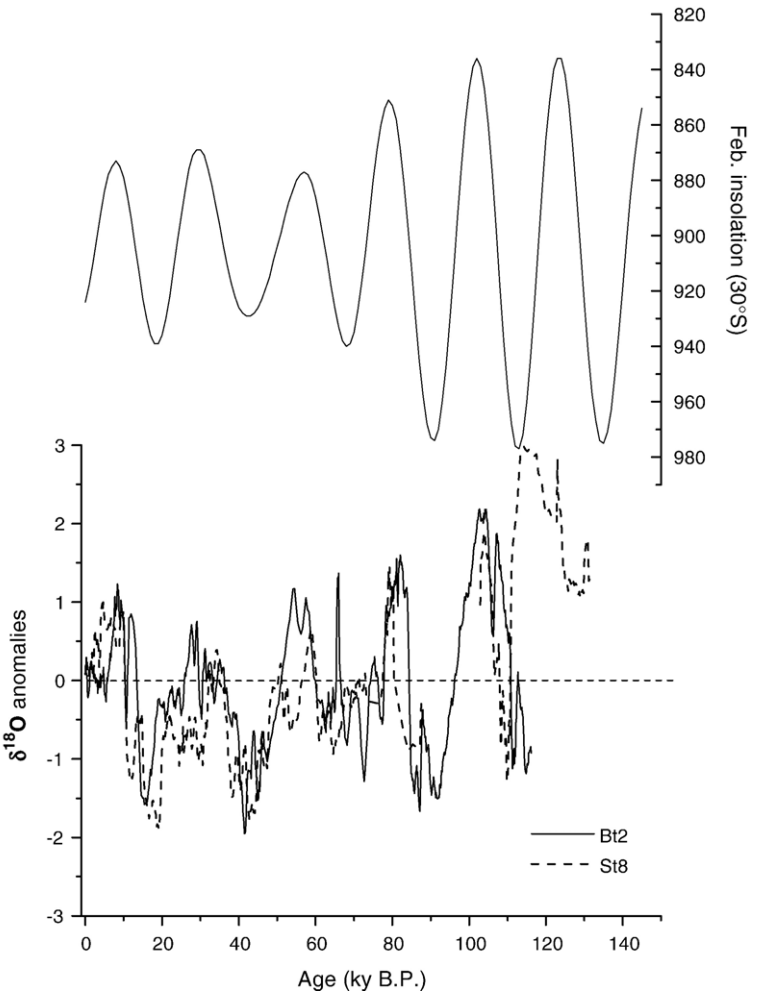

Fig. 7. February insolation at 30°S and $\delta^{18}O$ anomaly for Bt2 and St8 speleothems.

interval the anomaly peak is more positive than the insolation envelope and at the latter the negative anomalies are markedly dominant, even during the minima in insolation.

4. Discussion

As was the case for stalagmite Bt2, we interpret the oxygen isotope ratios of St8 to be primarily a function of rainfall moisture source during late Pleistocene. This interpretation requires that the calcite in St8 was deposited in or very near to isotopic equilibrium with the cave drip water. Isotopic equilibrium is evidenced by the lack of correlation between $\delta^{18}O$ and $\delta^{13}C$ along its growth axis ($r^2=0.003$) and present-day isotopic and climatic relationships obtained for the Santana cave system [2]. In addition, the relatively large range of variation in St8 $\delta^{18}O$ of about 7‰ suggests that temperature is not the dominant control on oxygen isotopic composition, as commonly observed in the sub(tropical) caves, because the fractionation factor between calcite and water is only −0.24‰/°C [16]. Therefore, we suggest that the isotopic signals in our speleothems are primarily a function of the relative contribution from distal (Amazon Basin) and local (Atlantic Ocean) sources, a feature closely linked to the variations in the meridional transport of air masses between tropical and midlatitudes. Increases and decreases in the isotopic values reflect higher proportions of extratropical and monsoonal precipitation infiltrating in the cave system, during the winter and summer periods, respectively.

Differences in the absolute isotopic ratios in the two speleothems are consistent with modern spatial $\delta^{18}O$ variability caused by latitudinal gradients in the dominant precipitation source. The $\delta^{18}O$ is always more depleted in St8 than in Bt2 by about 2‰, which implies that a steep latitudinal gradient of $\delta^{18}O$ persisted through the late

Quaternary. This is in agreement with the $\delta^{18}O$ composition of drip waters and modern speleothems from the study caves [2]. Systematic regional differences in mean absolute values and variations of $\delta^{18}O$ in our study are significantly higher than those observed in other speleothem studies performed in China [17] and in Israel [18,19]. This gradient is presumably maintained by a higher contribution of winter rainfall precipitation and a lower contribution of summer rainfall at Botuverá cave site than at Santana, as shown by modern climatology (Fig. 1). We argue that the differences in both mean values and short-term variations in $\delta^{18}O$ of our speleothems cannot be attributed to smoothing due to water mixing in relatively thick unsaturated zone because the variations of rainwater isotopic composition can be rapidly transmitted to the waters forming speleothems even at depths between 100 and 300 m [2].

Furthermore, it is interesting to note that the speleothem records present a striking similarity from 115 kyr BP to 60 kyr BP during the period of high amplitude of summer insolation but significant differences from 60 kyr BP to 10 kyr BP, a period when insolation shows much lower amplitude of variation (Fig. 7). The largest $\delta^{18}O$ differences between the two records are the result of negative anomalies in St8 during periods of lowest insolation, when one could expect positive anomalies. The seasonal patterns of mean precipitation could be altered by decreasing the relative amount of enriched rainfall during the winter or by a relative increase in depleted rainfall during the summer. The former case is unlikely to occur because the cyclonic events triggering the winter precipitation affect the sites to the same extent [4], while the latter is broadly consistent with the differences in summer rainfall variability over the region. Indeed it has been reported that positive anomalies in summer precipitation are at times limited to the area north of 25°S near the center of SACZ activity without a counterpart to the south of 25°S [11,20,21].

The $\delta^{18}O$ variations in both records cannot be explained solely in terms of insolation forcing alone. For example, anomalies at 45–39 kyr BP and 19–15 kyr BP are considerably more negative than those observed in other maxima in solar radiation at around 70 kyr BP and the present-day, although no significant differences in amplitude of insolation are observed in the last 70 kyr BP. Similarly, the anomalies at 32–25 kyr BP and at 8 kyr BP, during insolation minima, are quite different in magnitude. Other factors that could affect these anomalies are the atmosphere–ocean interactions in south Atlantic as reported by modern climatology [11,12] and a remote control by Northern Hemisphere glacial boundary conditions on the ITCZ position [22]. We exclude the first possibility because unlike the $\delta^{18}O$ in the speleothems, SSTs in the South Atlantic do not show significant variations over this time period [23]. The second factor is more likely because an ITCZ positioned farther south could enhance the moisture supply and lead to more intense convection over the Amazon Basin. The coincidence of greatest negative anomalies in both records with the timing of Heinrich events supports this interpretation. Most of the negative anomalies in our records are also coincident with pluvial events recorded by speleothem growth in Northeastern Brazil [24]. For example negative anomalies at around 110 kyr BP, 88 kyr BP, 60–70 kyr BP, 40 kyr BP and 15 kyr BP all coincide with speleothem growth in northeastern Brazil [24].

Wang et al. suggested that the confluence of Heinrich events and maxima in Southern Hemisphere summer insolation resulted in southerly shifts in the location of the ITCZ, which brought greatly increased rainfall to northeast Brazil. Similarly, the increased ice volume and decreased temperature in the high northern latitudes during Heinrich events result in a greater contribution of summer rainfall to our study area beyond the variations imposed by changes in Southern Hemisphere summer insolation alone [1]. In addition, our data suggest that Northern Hemisphere ice volume and temperatures not only influence the mean position of the ITCZ but also result in a shift in the mean position of the SACZ.

The relatively low $\delta^{18}O$ values observed in our records from 60 kyr BP to 19 kyr BP indicate that Northern Hemisphere ice volume and temperature influence SASM/SACZ activity in the region for this entire period, resulting in more persistent summer rainfall even during S.H. low insolation phases. This interpretation is in agreement with the wettest conditions recorded at the same period in Salar de Uyuni, an area in the Bolivian Altiplano where precipitation equally depends on SASM activity [25].

The St8 stalagmite provides information on climate during the last interglacial period in South America, which has not yet been documented in other absolutely dated records over the continent except for the Salar de Uyuni record [25]. In our data, this period is marked by a dominance of extratropical over monsoonal precipitation, as interpreted from the remarkably enriched $\delta^{18}O$ values of St8 starting at the stalagmite bottom at approximately 131 kyr BP until about 118 kyr BP. The $\delta^{18}O$ variations can be separated into two phases throughout this period: a first phase from 131 to ~125 kyr BP with values at a level of −3.9‰, that are substantially more enriched than the record mean (−5.08‰) and a second phase marked by values above −3‰, which are the maximum values found in the record (Fig. 6). The last phase starts abruptly at ~125 and terminates at ~112 kyr BP.

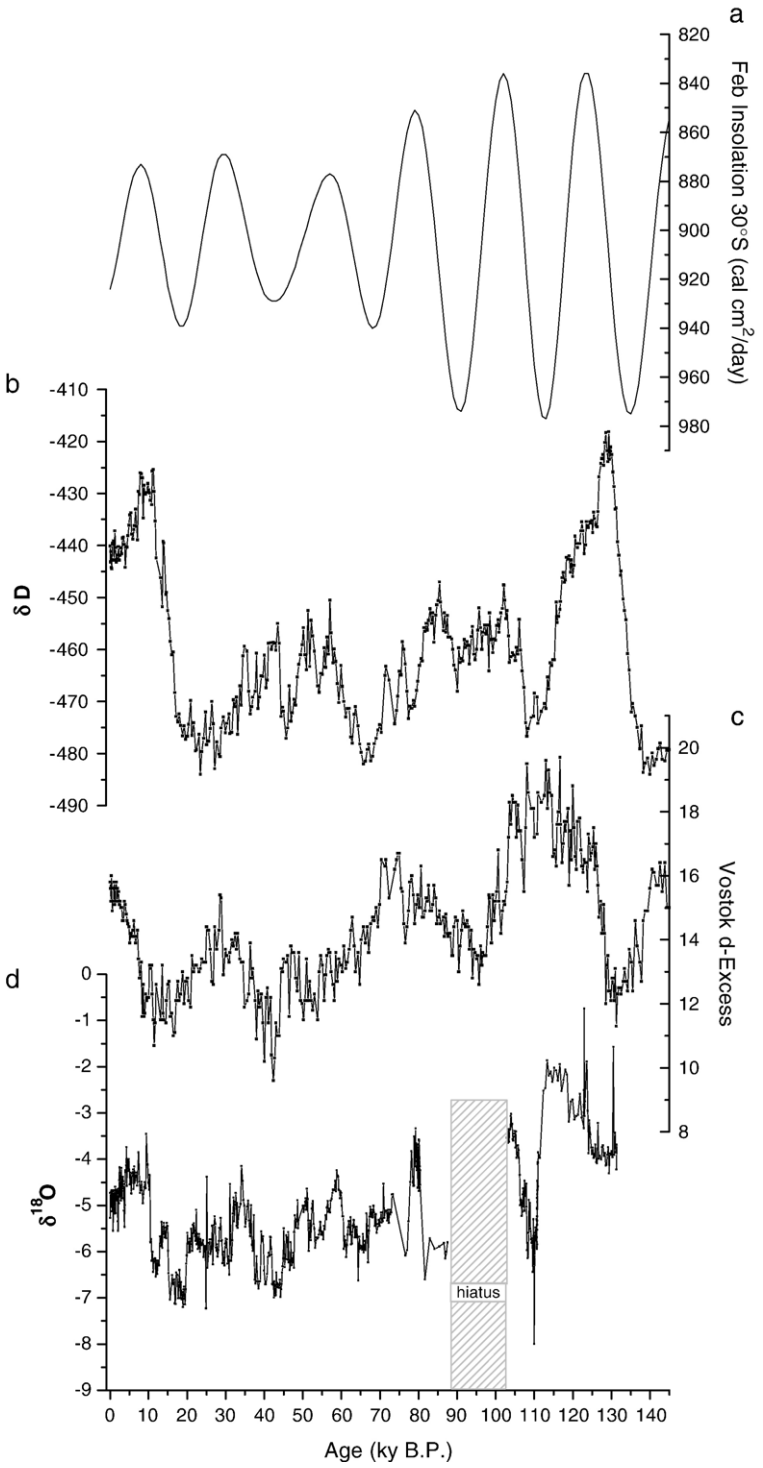

Fig. 8. Comparison between (a) February insolation at 30°S; (b) Vostok deuterium from Antarctica [31]; (c) Vostok deuterium excess [27]; (d) oxygen isotopes of St8.

The timing and pattern of climate variation observed in the St8 record is quite different from most other climate records for this time period. The peak last interglacial period, in terms of temperature and sea level, is generally considered to be from 130 kyr BP to 120 kyr BP, with perhaps an error on either of these two dates of about 1000 yrs [26]. Thus, we would expect a transition from less to more negative $\delta^{18}O$ values to occur in St8 at about 120 kyr BP in response to both increasing Southern Hemisphere summer insolation and decreasing Northern Hemisphere temperatures. These factors should act to move the ITCZ south during the transition from MIS 5e to 5d. Instead, a very large, rapid decrease in St8 $\delta^{18}O$ occurs much later at ~112 kyr BP. Interestingly, the pattern found in the St8 isotopic record during this time is similar to the deuterium excess record from the Vostok ice core (Fig. 8).

We argue that the $\delta^{18}O$ anomalies during the optimum of the last interglacial period in Brazil are too high to be caused only by insolation and that other factors should be also considered (Fig. 7). The mechanism explaining this additional increase in $\delta^{18}O$ and hence in winter precipitation must be related to an enhancement of the extratropical circulation, probably induced by higher meridional temperature/pressure gradients. In the Vostok ice core, the high deuterium-excess observed between 126 and 103 kyr BP (Fig. 8) has been interpreted in a similar way [27]. This mechanism is also consistent with the fact that both water vapor transport toward Antarctica and the dynamics of the winter precipitation regime over the Brazilian subtropics are strongly influenced by meridional shifts of the atmospheric circulation over the Southern Hemisphere.

5. Conclusions

A comparison of the oxygen isotope ratios between the two stalagmites from southern and southeastern Brazil, St8 and Bt2, shows a good match between the two records and indicates a dominant control of summer insolation on long-term seasonal changes in rainfall over subtropical Brazil. However, it is also clear that significant differences in the $\delta^{18}O$ mean values and variability occur on both long-term and millennial times scales. Higher values of $\delta^{18}O$ in Bt2 than in St8 are consistent with the results of modern monitoring of drip waters and modern speleothems from the two caves [2] and suggest that a steep gradient of $\delta^{18}O$ has been maintained in the region since 116 kyr BP due to more abundant enriched extratropical and depleted monsoonal rainfall at the southern and northern cave site, respectively. The last interglacial period is marked by highest values of $\delta^{18}O$ in St8 and indicates a typical extratropical regime with rainfall events occurring mainly in the winter.

The analysis of $\delta^{18}O$ anomalies from our speleothems demonstrates that summer insolation cannot explain all the negative anomalies observed in the record. We consider that part of these anomalies resulted from an additional control exerted by the Northern Hemisphere glacial boundary conditions, in particular during Heinrich events, on the SASM by displacing the SACZ further south than could be expected by insolation forcing alone. This information can be fundamental for understanding the factors controlling the past activity of SASM. In addition, the presence or absence of millennial-scale events and the differences in their magnitude in subtropical Brazil highlight their dependence on regional climate factors such as differences in seasonal rainfall distribution. These results suggest that caution is needed when interpreting the intensity and global extension of abrupt climate events in the Southern Hemisphere without making a regional comparison. In some cases the response of the climate system to a specific event can differ from place to place due to the influence of local climate factors.

Acknowledgement

We thank the Fundação de Amparo a Pesquisa do Estado de São Paulo (FAPESP), Brazil, for financial support of this research (Grant 99/10351-6 to I. Karmann and scholarship to F.W. Cruz, Jr.). We are grateful to Françoise Vimeux for providing the deuterium excess data set of Vostok ice core. We thank the helpful comments and suggestions by two anonymous reviewers. We thank to Ray Bradley for revising the manuscript. The field work and stalagmite collection was executed with authorization of Brazilian environmental Department administration, IBAMA/CECAV and PETAR State Park. We thank Jurandir Santos and Wanderley Saturnino (*in memoriam*) for helping us in the field.

References

[1] F.W. Cruz, S.J. Burns, I. Karmann, W.D. Sharp, M. Vuille, A.O. Cardoso, J.A. Ferrari, P.L. Silva Dias, O. Viana Jr., Insolation-driven changes in atmospheric circulation over the past 116,000 years in subtropical Brazil, Nature 434 (2005) 63–66.

[2] F.W. Cruz, I. Karmann, O. Viana Jr., S.J. Burns, J.A. Ferrari, M. Vuille, A.N. Sial, M.Z. Moreira, Stable isotope study of cave percolation waters in subtropical Brazil: implications for paleoclimate inferences from speleothems, Chem. Geol. 220 (2005) 245–262.

[3] M.A. Gan, V.B. Rao, Surface cyclogenesis over South America, Mon. Weather Rev. 119 (1991) 1293–1302.

[4] C.S. Vera, P.K. Vigliarolo, E.H. Berbery, Cold season synoptic-scale waves over subtropical South America, Mon. Weather Rev. 130 (2002) 684–699.

[5] J. Zhou, K.M. Lau, Does a monsoon climate exist over South America? J. Clim. 11 (1998) 1020–1040.
[6] M.A. Gan, V.E. Kousky, C.F. Ropelewski, The South American monsoon circulation and its relationship to rainfall over West-Central Brazil, J. Clim. 17 (2004) 47–66.
[7] L.M.V. Carvalho, C. Jones, B. Liebmann, The South Atlantic Convergence Zone: intensity, form, persistence, and relationships with intraseasonal to interannual activity and extreme rainfall, J. Clim. 17 (2004) 88–108.
[8] R.D. Garreaud, J.M. Wallace, Summertime incursions of midlatitude air into subtropical and tropical South America, Mon. Weather Rev. 126 (1998) 2713–2733.
[9] M. Vuille, R.S. Bradley, M. Werner, R. Healy, F. Keimig, Modeling $\delta^{18}O$ in precipitation over the tropical Americas: 1. Interannual variability and climatic controls, Journal of Geophysical Research 108 (D6) (2003) 4174, doi:10.1029/2001JD002038.
[10] M. Vuille, M. Werner, Stable isotopes in precipitation and the South American summer monsoon – observations and model results, Clim. Dyn. 25 (2005) 401–413, doi:10.1007/500382-005-0049-9.
[11] A.W. Robertson, C.R. Mechoso, Interannual and interdecadal variability of the South Atlantic convergence zone, Mon. Weather Rev. 128 (2000) 2947–2957.
[12] J.N. Paegle, K.C. Mo, Linkages between summer rainfall variability over South America and sea surface temperature anomalies, J. Clim. 15 (2002) 1389–1407.
[13] G.C. Campanha, G.R. Sadowski, Tectonics of the southern portion of Ribeira Belt (Apiaí Domain), Precambrian Res. 98 (1999) 31–51.
[14] V.B. Rao, K.V. Hada, Characteristics of rainfall over Brazil: annual variations and connections with the Southern Oscillation, Theor. Appl. Climatol. 42 (1990) 81–90.
[15] IAEA/WMO, Global Network for Isotopes in Precipitation (GNIP) Database. IGBP PAGES/World Data Center-A for Paleoclimatology Data Contribution Series # 94-005. NOAA/NGDC Paleoclimatology Program, Boulder CO, USA, 1994.
[16] I. Friedman, J.R. O'Neil, Compilation of stable isotope fractionation factors of geochemical interest, Data of Geochemistry, United States Geological Survey Professional Paper 440-KK, 1977, pp. 1–12.
[17] D. Yuan, H. Cheng, R.L. Edwards, C.A. Dykoski, M.J. Kelly, M. Zhang, J. Qing, Y. Lin, Y. Wang, J. Wu, J.A. Dorale, Z. An, Y. Cai, Timing, duration, and transitions of the last interglacial Asian monsoon, Science 304 (2004) 575–578.
[18] M. Bar-Matthews, A. Ayalon, M. Gilmour, A. Matthews, C.J. Hawkesworth, Sea–land oxygen isotopic relationships from planktonic foraminifera and speleothems in the Eastern Mediterranean region and their implication for paleorainfall during interglacial intervals, Geochim. Cosmochim. Acta 67 (2003) 3181–3199.
[19] A. Vaks, M. Bar-Matthews, A. Ayalon, B. Schilman, M. Gilmour, C.J. Hawkesworth, A. Frumkin, A. Kaufman, A. Matthews, Paleoclimate reconstruction based on the timing of speleothem growth and oxygen and carbon isotope composition in a cave located in the rain shadow in Israel, Quat. Res. 59 (2003) 182–193.
[20] J. Nogués-Paegle, K.C. Mo, Alternating wet and dry conditions over South America during summer, Mon. Weather Rev. 125 (1997) 279–291.
[21] A. Díaz, P. Aceituno, Atmospheric circulation anomalies during episodes of enhanced and reduced convective cloudiness over Uruguay, J. Clim. 16 (2003) 3171–3186.
[22] J.C.H. Chiang, M. Biasutti, D.S. Battisti, Sensitivity of the Atlantic Intertropical Convergence Zone to the last glacial maximum boundary conditions, Paleoceanography 18 (4) (2003) 1094, doi:10.1029/2003PA000916.
[23] H. Arz, Dokumentation von kurzfristigen Klimaschwankungen des Spätquartärs in Sedimenten des westlichen äquatorialen Atlantiks, Ber. Fachbereich Geowiss. Univ. Brem. 124 (1998) 96 pp.
[24] X. Wang, A.S. Auler, R.L. Edwards, H. Cheng, P.S. Cristalli, P.L. Smart, D.A. Richards, C.-C. Shen, Wet periods in northeastern Brazil over the past 210 kyr linked to distant climate anomalies, Nature 432 (2004) 740–743.
[25] S.C. Fritz, P.A. Baker, T.K. Lowenstein, G.O. Seltzer, C.A. Rigsby, G.S. Dwyer, P.M. Tapia, K.K. Arnold, T-L. Ku, S. Luo, Hydrologic variation during the last 170,000 years in the Southern Hemisphere tropics of South America, Quat. Res. 61 (2004) 95–104.
[26] G.J. Kukla, et al., Last interglacial climates, Quat. Res. 58 (2002) 2–13.
[27] F. Vimeux, V. Masson, J. Jouzel, M. Stievenard, J.R. Petit, Glacial–interglacial changes in ocean surface conditions in the Southern Hemisphere, Nature 398 (1999) 410–413.
[28] P. Xie, P.A. Arkin, Global precipitation: a 17-year monthly analysis based on gauge observations, satellite estimates, and numerical model outputs, Bull. Am. Meteorol. Soc. 78 (1997) 2539–2558.
[29] A. Berger, M.F. Loutre, Insolation values for the climate of the last 10 million of years, Quat. Sci. Rev. 10 (1991) 297–317.
[30] North Greenland Ice Core Project members, High resolution record of Northern Hemisphere climate extending into the last interglacial period, Nature 431 (2004) 147–151.
[31] J.-R. Petit, J. Jouzel, D. Raynaud, N.I. Barkov, J.-M. Barnola, I. Basile, M.L. Bender, J. Chappellaz, M.E. Davis, G. Delaygue, M. Delmotte, V.M. Kotlyakov, M. Legrand, V.Y. Lipenkov, C. Lorius, L. Pépin, C. Ritz, E. Saltzman, M. Stievenard, Climate and atmospheric history of the past 420,000 years from the Vostock ice core, Antarctica, Nature 399 (1999) 429–436.